Biocompatible Inorganic Fullerene-Like Molybdenum Disulfide Nanoparticles Produced by Pulsed Laser Ablation in Water

Haihua Wu,[†] Rong Yang,[†,*] Baomin Song,[†] Qiusen Han,[†] Jingying Li,[†] Ying Zhang,[†] Yan Fang,[‡] Reshef Tenne,[§] and Chen Wang[†,*]

[†]CAS Key Lab for Biomedical Effects of Nanomaterials and Nanosafety, National Center for Nanoscience and Technology, Beijing, 100190, People's Republic of China, [‡]Department of Physics, Capital Normal University, Beijing, 100037, People's Republic of China, and [§]Department of Materials and Interfaces, Weizmann Institute of Science, Rehovot 76100, Israel

ABSTRACT We report on the synthesis of inorganic fullerene-like molybdenum disulfide (MoS_2) nanoparticles by pulsed laser ablation (PLA) in water. The final products were characterized by scanning electron microscopy, X-ray diffraction, transmission electron microscopy, and resonance Raman spectroscopy, *etc.* Cell viability studies show that the as-prepared MoS_2 nanoparticles have good solubility and biocompatibility, which may show a great potential in various biomedical applications. It is shown that the technique of PLA in water also provides a green and convenient method to synthesize novel nanomaterials, especially for biocompatible nanomaterials.

KEYWORDS: colloids · inorganic fullerene-like · biomedical applications · nanoparticles · pulsed laser ablation · biocompatibility

There has been a lot of interest in the study of nanostructures due to their unique properties and potential applications in new nanotechnologies.[1−5] Molybdenum disulfide (MoS_2), tungsten disulfide (WS_2), and layered inorganic compounds were found to have a comparable structure to carbon nanoparticles, *i.e.*, hollow cage structure, like carbon "onions", and nanotubes and could form inorganic fullerene-like (termed IF) structures under appropriate conditions.[6−11] MoS_2 and WS_2 nanostructures have distinctive properties (like excellent lubrication properties)[12] and wide ranges of promising applications, such as heterogeneous catalysis, hydrogen storage, and lithium−magnesium ion batteries, *etc.*[9−11] The first potential medical application—alleviating friction in orthodontic wires—was recently demonstrated.[12−14] Furthermore, self-lubricating friction-reduction coatings with possible biomedical potential based on MoS_2 and WS_2 nanoparticles with inorganic fullerene-like (IF) structure, such as coatings for artificial joints, have been suggested by Samorodnitzky-Naveh *et al.*[14] They showed that stable and well-adhered cobalt + IF-WS_2 coating of NiTi substrates was obtained. Friction tests presented up to 66% reduction of the friction coefficient. Since NiTi alloy is widely used for many medical appliances, this unique friction-reducing coating could be implemented to provide better manipulation. In addition, biofunctionalization of WS_2 nanostructures has also been achieved by Tahir *et al.*[15] They have used a polymeric ligand containing the tetradentate nitrilotriacetic acid (NTA) groups with dual functionality to anchor functional groups to the surface sulfur layer and the linker groups for biofunctionalization through the immobilization of His-tagged protein (silicatein) to the functionalized chalcogenide surface. The protein retains its catalytic activity when immobilized on the surface of WS_2 nanotubes. Biofunctionalization of WS_2 nanostructures opens new opportunities for integrating this group of nanomaterials in composites, especially for immobilization of various proteins and biomolecules. All these progresses make metal chalcogenide nanoparticles good candidates for various biomedical applications, such as drug delivery (through controlled release of small molecules or proteins),[15] cancer therapy, and medical-relevant coatings.

Before any material can be used for biomedical applications, its biocompatibility and toxicology must be evaluated. Preliminary toxicology tests of WS_2 nanoparticles revealed that the material showed no apparent toxic reaction after an oral administration test in rats and no sensitization in lymph nodes following a topical dermal application.[16,17] More recent inhalation tests have shown that the material has no toxic effect in rats.[18] Nevertheless more toxicity

*Address correspondence to yangr@nanoctr.cn, wangch@nanoctr.cn.

Received for review October 31, 2010 and accepted December 26, 2010.

Published online January 11, 2011
10.1021/nn102941b

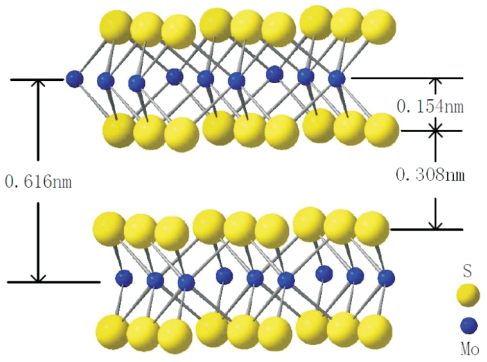

Figure 1. Schematic diagram of the 2H-MoS_2 structure. (The lattice parameters in figure were taken from ref 29).

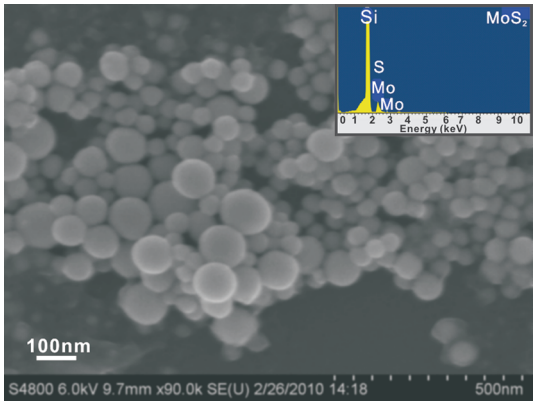

Figure 2. The FE-SEM image of MoS_2 nanoparticles and the EDS spectrum in the inset.

and sensitivity tests need to be done in view of the emerging applications of these nanomaterials.

Up to now, much effort has been devoted to the synthesis of these novel nanostructures. Various methods have been reported,[19−26] such as the gas-phase reaction between oxides and H_2S/H_2,[20,21] decomposition of ammonium thiomolybdate or metal trisulfides,[22,23] heating of MoS_2 powders,[24] and the catalyzed transport method, *etc.*[25] In this work, we use pulsed laser ablation (PLA) to prepare MoS_2 nanoparticles in deionized water. PLA in water is a relatively new method[27,28] to prepare the metal and semiconductor nanoparticles, and it is also a potentially important method to produce nanoparticles which could be used in drug delivery and other biomedical applications. Compared with chemical methods, PLA in water can produce nanoparticles with several advantages: (1) Preparation is relatively simple and convenient; (2) the nanoparticle system is pure without other remnants from the chemical reactions; and (3) the products have high water solubility.

Here, we report on the synthesis of IF-MoS_2 nanoparticles by PLA of pressed pellets of 2H-MoS_2 powder in water. The final products were characterized by field emission scanning electron microscopy (FE-SEM), X-ray diffraction (XRD), transmission electron microscopy (TEM), and resonance Raman Spectroscopy, *etc.* Cell viability studies were conducted with the IF-MoS_2 nanoparticles and different human cells. The IF-MoS_2 nanoparticles were found to be nontoxic to these cells up to the stated concentrations.

RESULTS AND DISCUSSION

Figure 1 shows the structure of bulk MoS_2 crystal,[29] which contains a Mo layer sandwiched between two S layers with the Mo in a trigonal biprism coordination. Strong covalent forces bind Mo and S atoms within a lamella, whereas adjacent lamellae interact through relatively weak van der Waals forces. The unit cell has hexagonal symmetry and includes two adjacent lamellae (termed 2H arrangement). This graphite-like structure is considered to be responsible for the lubricative properties of these materials, because the weak interlamellar forces facilitate the shear when the direction of sliding is parallel to the planes of the material.

Figure 2 shows a SEM image of MoS_2 nanoparticles prepared by PLA in water. The starting material was a pressed pellet of MoS_2 powder. A series of analytical experiments was carried out in order to determine the composition and structure of the generated nanoparticles. One can see that the product consists of spherical nanoparticles. The average diameter of the MoS_2 nanoparticles is about 120 nm, as determined by dynamic light scattering (DLS) measurement (Supporting Information, Figure S2). Energy-dispersive X-ray spectrum (EDS, Horiba, installed on SEM) shows that the nanoparticles primarily contain Mo and S. (Figure 2 inset, the Si peak in the figure comes from the Si substrate).

XRD measurements were carried out to determine the structure and composition of the MoS_2 nanoparticles, and the result is shown in Figure 3. It can be observed that all the diffraction peaks in spectrum (a) can be indexed to MoS_2 with hexagonal structure (ICDD-JCPDS card no. 39-1492). In comparison, Figure 3b shows the XRD pattern of the 2H-MoS_2 powder. All the peaks in spectrum (b) can be assigned to the hexagonal 2H-MoS_2 with lattice constants a = 3.160, c = 12.295 Å (ICDD-JCPDS card no. 39-1492). One can see that the main peaks, *i.e.*, (002) and (006) in Figure3a exhibit a small shift to lower angles compared to their corresponding ones in Figure3b, which indicated about 0.3% lattice expansion. This shift can be attributed to the introduction of strain owing to curvature of the layers.[30]

Figure 4 shows a typical high-resolution TEM (HRTEM) image of MoS_2 nanoparticles prepared by PLA in water. The layered structure of the walls forming these fullerene-like nanoparticles is quite clear from the image. The interlayer distance is about 6.18 Å, which corresponds to the d-spacing of MoS_2 (002) planes. The inset in Figure 4 is a line profile of the boxed region.

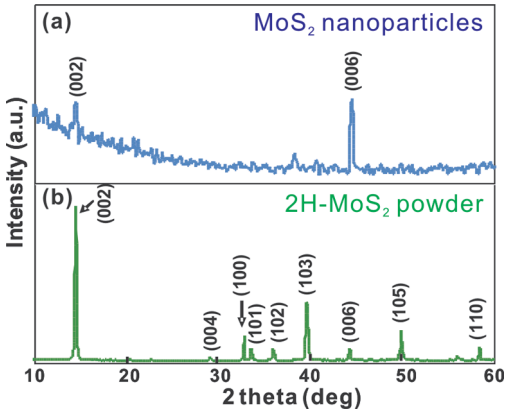

Figure 3. XRD patterns for: (a) MoS_2 nanoparticles and (b) 2H-MoS_2 powder.

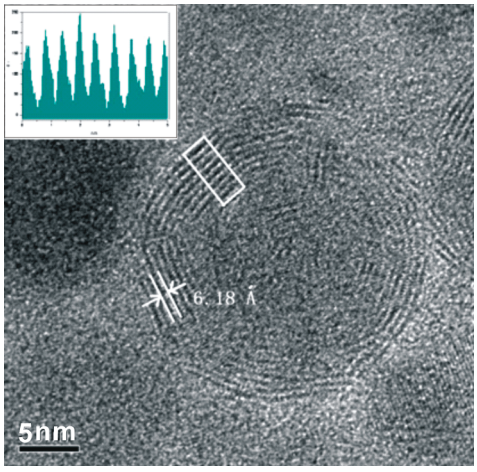

Figure 4. HRTEM image of MoS_2 nanoparticles.

Resonance Raman (RR) spectra of IF-MoS_2 nanoparticles and 2H-MoS_2 powder are shown in Figure 5, which were taken at room temperature using the 632.8 nm He−Ne laser excitation line. The modes shown in Figure 5 are listed in Table 1. In the RR spectrum of the 2H-MoS_2 powder, many peaks are observed. All the peaks are in good agreement with the reported MoS_2 single-crystal resonance Raman studies.[31,32] In the RR spectrum of IF-MoS_2 nanoparticles, the most intense peak is centered at 405 cm^{-1}. This mode is assigned to the $A_{1g}(\Gamma)$ mode.[31,32] In the higher frequency region of the RR spectrum, peaks are observed at 593 and 638 cm^{-1}, which were assigned to the second-order processes: E^1_{2g} (M) + LA(M) and A_{1g}(M) + LA(M), respectively. In the lower frequency region of the RR spectrum, there are two peaks at 175 and 378 cm^{-1}, which were assigned to the A_{1g}(M) − LA(M) and $E^1_{2g}(\Gamma)$, respectively. All the RR peaks of MoS_2 nanoparticles in Figure 5 shift to lower frequencies compared to their bulk ones, which is a typical phenomenon observed in MoS_2 nanostructures.[32−34] (The peak at 520 cm^{-1} comes from the Si substrate.)

One can also see from Figure 5 that the most intense peak in the RR spectrum of the 2H-MoS_2 powder is

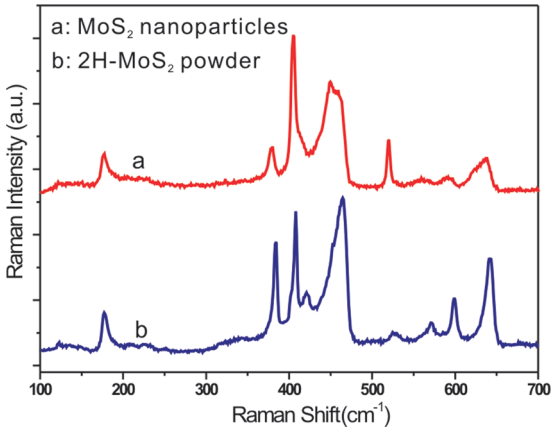

Figure 5. RR spectra of MoS_2 nanoparticles and 2H-MoS_2 powder.

TABLE 1. Raman Peaks Observed in MoS_2 Samples at Room Temperature and Corresponding Symmetry Assignments[a]

MoS_2 powder	IF-MoS_2	symmetry assignment
176	175	A_{1g}(M) − LA(M)
384	378	$E^1_{2g}(\Gamma)$
408	405	$A_{1g}(\Gamma)$
421		
	450	
464	463	2 × LA(M)
524		E_{1g}(M) + LA(M)
571		2 × $E_{1g}(\Gamma)$
602	593	E^1_{2g}(M) + LA(M)
643	638	A_{1g}(M) + LA(M)

[a] All peak positions are in cm^{-1}. LA refers to longitudinal acoustic, Γ and M refer to Γ and M points in the electronic-band structure diagrams.

centered at 464 cm^{-1}. This mode has been previously assigned by Stacy *et al.*[31] to the second-order 2 × LA(M) mode. In the spectrum of MoS_2 nanoparticles, this peak is actually split into two peaks at 450 and 463 cm^{-1}, suggesting that this feature is a superposition of two peaks. Figure S3a, Supporting Information, shows that the fitted data and Lorentzian functions are used to deconvolute the feature into two peaks. The relative intensity, *P*(low peak)/*P*(high peak), is larger for the sample of nanoparticles than that for the sample of the 2H-MoS_2 powder, which is in agreement with the results of Frey *et al.*[32]

In light of these results, the formation mechanism of fullerene-like MoS_2 can be discussed. This process involves the interaction between pulsed laser radiation and the target source material. Stresses produced by laser-induced thermal shock were not relieved and could eventually lead to cracking and flake detachment, *i.e.*, "exfoliation".[35] Laser exfoliation caused the delamination of nanosize layer structured MoS_2 materials. The ejected MoS_2 thin flakes and fragments were hit by shock waves produced during subsequent pulses, causing further diminution of particles. SEM images of the

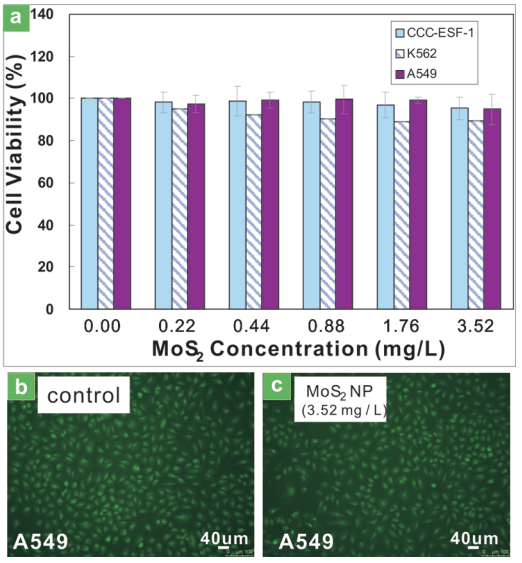

Figure 6. (a) Cell viability of different cells (A549, K562, and CCC-ESF-1) after incubating in increasing concentrations of MoS_2 nanoparticles, as determined by the MTT test. (b and c) fluorescent microscopy images of untreated control A549 cells and the cells treated with MoS_2 nanoparticles (3.52 mg/L) for 48 h, respectively.

starting MoS_2 powder and the IF-MoS_2 nanoparticles produced by PLA in water for 10 min are shown in Figure S5, Supporting Information. One can notice from that the sizes of those MoS_2 nanoparticles are larger than those ablated for 20 minutes, which also supports this explanation.

The use of nanoparticles *in vitro* and *in vivo* requires that they are biocompatible. The cytotoxic behavior of MoS_2 nanoparticles on cells was examined by the MTT (3-(4,5-dimethylthiazol-2-yl)-2,5-diphenyltetrazolium bromide) assay. CCC-ESF-1 cell (human embryonic epidermal fibroblast cells) viability was assessed 48 h after exposure to different concentrations of MoS_2 nanoparticles. Control experiments were conducted in a similar manner without the presence of the MoS_2 nanoparticles. As shown in Figure 6a, cell viability data indicated that the MoS_2 nanoparticles did not significantly affect CCC-ESF-1 cell proliferation up to 3.52 mg/L particle concentration. In order to compare different cell viability in the presence of MoS_2 nanoparticles, we have tested two other different human cells: A549 cells (lung adenocarcinoma cells) and K562 cells (leukemic cells). The results showed that the MoS_2 nanoparticles were reasonably nontoxic and biocompatible up to the given concentrations.

To study further the effect of MoS_2 nanoparticles on cell viability, we labeled A549 cells with acridine orange (Sigma Aldrich) and studied the cell morphologies under a fluorescent microscope. A549 cells were cultured in 96-well plates and incubated with MoS_2 nanoparticles with various concentrations, as discussed above. Figure 6b shows the fluorescent microscopy images of untreated control A549 cells and the cells treated with MoS_2 nanoparticles (3.52 mg/L) for 48 h. In acridine orange-stained cells, the nucleolus fluorescence was bright green, but the cytoplasm was a little dim. There was no obvious change of the morphologies after treatment with the MoS_2 nanoparticles for 2 days even at the highest concentration. There was nevertheless a little decrease in the cell numbers, which was similar to the case for the untreated cells. In conclusion we found that the MoS_2 nanoparticles were nontoxic to the cells at the given concentrations. It is interesting to compare cytotoxic effects of MoS_2 nanoparticles with those of other nanomaterials, such as single-walled carbon nanotube (SWCNT) particles. It was found by Manna *et al.*[36] that cell survival started to decrease after exposure to low concentration (0.15 mg/L) of SWCNT particles. Thus, MoS_2 nanoparticles seem to have a very good biocompatibility with the above human cells.

CONCLUSION

In summary, we prepared fullerene-like MoS_2 nanoparticles using PLA in water. The structure of the products was characterized by SEM, EDS, XRD, TEM, and Raman spectroscopy techniques. A mechanism for the nanoparticle synthesis was proposed. Cell viability studies show that the as-prepared MoS_2 nanoparticles have good solubility and biocompatibility, which may have an important impact on variety of applications, including various biomedical applications, such as medical friction-reduction coatings, drug delivery, and cancer therapy. The technique of PLA in water also provides a green and convenient method to synthesize novel crystalline materials, especially for biocompatible nanomaterials.

MATERIALS AND METHODS

Synthesis of MoS_2 Nanoparticles. Synthesis of MoS_2 nanoparticles was carried out by using PLA in water. The MoS_2 powder (Sigma Aldrich, 99.99% pure) was pressed into a target pellet (diameter of 15 mm) using a press system for infrared spectroscopy (a pressure of 12 MPa, 2 min). The pellet was placed at the bottom of a quartz cell with 5 mL redistilled deionized water. A Nd:YAG pulsed laser (532 nm, 5 Hz, pulse duration between 6 and 9 ns and pulse energy of 40−50 mJ), was focused on the MoS_2 pellet for ablation. The ablation was typically done for duration of 20 min. During the course of the ablation, the colloidal solution was continuously stirred by a magnetic stirrer.

Characterization. The MoS_2 nanoparticles were filtered with 0.45um disposable filters and then characterized by FE-SEM (Hitachi S-4800), EDS (Horiba), TEM (Tecnai G220 ST), RR spectroscopy (Renishaw, the excitation wavelength was 632.8 nm), DLS (Malvern Zetasizer Nano ZS), and XRD (Bruker D8). The concentrations of the MoS_2 nanoparticle colloid solution used for the cell viability studies were measured with optical emission spectroscope of inductively coupled plasma ICP-OES (Perkin-Elmer optima 5300DV).

Cell Culture. A549 and K562 cells were cultured in RPMI 1640 medium (Thermo Scientific) (CCC-ESF-1 cells were cultured in DMEM/high glucose medium) with 10% (V/V) fetal bovine serum (FBS) and 100 IU/mL penicillin and 100 μg/mL streptomycin, respectively. The culture plates were incubated at 37 °C in a humidified incubator containing 5% CO_2.

MTT Assay for Cell Viability Test. The cell viability was tested using MTT assay, which is based on the mitochondrial conversion of tetrazolium salt. The A549 and K562 cells were seeded in 96-well microplates (Costar, Corning, NY) at a density of 8000 and 1.0 $\times$ 10^4cells/well, respectively, in 100 μL RPMI 1640 medium containing 10% FBS. CCC-ESF-1 cells were seeded at a density of 1.0 $\times$ 10^4cells/well in DMEM/high-glucose medium. After attachment for 24 h, the cells were incubated with MoS_2 nanoparticles at various concentrations (0, 0.22, 0.44, 0.88, 1.76, and 3.52 mg/L) for another 48 h in a final volume containing 150 μL medium, and then the medium was removed (except for experiments of K562 cells). After that, 150 μL of fresh medium and 10 μL of MTT (5 mg/mL in PBS) were added to each well, and the culture plates were incubated at 37 °C and 5% CO_2 for 4 h. After removal of the medium, 150 μL of dimethyl sulfoxide (DMSO) was added to each well to dissolve the dye. The absorbance at 492 nm was measured using a microplate reader. Each data point was derived from three parallel samples.

Cell Viability Assay by Fluorescent Microscopy. The A549 cells were cultured in 96-well plates and mixed with MoS_2 nanoparticles, as discussed above. After treatment, the cells were labeled by incubation with acridine orange (Sigma Aldrich) at a concentration of 100 ug/mL for 20 min at 37 °C in the dark. After incubation, the cells were washed twice with ice-cold complete medium and examined under a fluorescent microscope (Leica, Germany). Three sections were selected and examined randomly for each sample. Excitation was performed by an argon ion laser operating at 488 nm, and the emitted fluorescence was collected through a 515 nm pass filter.

Acknowledgment. This work was supported by National Natural Science Foundation of China (20911130229, 21073047), the Chinese Academy of Sciences (KJCX2.YW.M15), and the "863" Program of the Ministry of Science and Technology (2009AA03Z335).

Supporting Information Available: Schematic diagram of the experimental setup, DLS of MoS_2 nanoparticles, a line-shape analysis of the 440−470 cm^{-1} feature in the resonance Raman spectra of MoS_2 nanoparticles and powders, a HRTEM image of the MoS_2 nanoparticles, and FE-SEM images of MoS_2 powder and MoS_2 nanoparticles produced by PLA in water for 10 min. This material is available free of charge *via* the Internet at http://pubs.acs.org.

REFERENCES AND NOTES

1. Qing, Q.; Pal, S. K.; Tian, B.; Duan, X.; Timko, B. P.; Cohen-Karni, T.; Murthy, V. N.; Lieber, C. M. Nanowire Transistor Arrays for Mapping Neural Circuits in Acute Brain Slices. *Proc. Natl. Acad. Sci. U.S.A.* **2010,** *107*, 1882–1887.
2. Rao, C. N. R.; Govindaraj, A. Synthesis of Inorganic Nanotubes. *Adv. Mater.* **2009,** *21*, 4208–4233.
3. Lauritsen, J. V.; Kibsgaard, J.; Helveg, S.; Topsoe, H.; Clausen, B. S.; Legsgaard, E.; Besenbacher, F. Size-dependent Structure of MoS_2 Nanocrystals. *Nat. Nanotechnol.* **2007,** *2*, 53–58.
4. Tenne, R. Inorganic Nanotubes and Fullerene-like Nanoparticles. *Nat. Nanotechnol.* **2006,** *1*, 103–111.
5. Cho, E. C.; Camargo, P. H. C.; Xia, Y. Synthesis and Characterization of Noble-Metal Nanostructures Containing Gold Nanorods in the Center. *Adv. Mater.* **2010,** *22*, 744–748.
6. Tenne, R.; Margulis, L.; Genut, M.; Hodes, G. Polyhedral and Cylindrical Structures of Tungsten Disulphide. *Nature* **1992,** *360*, 444–446.
7. Li, Y. D.; Wang, J. W.; Deng, Z. X.; Wu, Y. Y.; Sun, X. M.; Yu, D. P.; Yang, P. D. Bismuth Nanotubes: A Rational Low-Temperature Synthetic Route. *J. Am. Chem. Soc.* **2001,** *123*, 9904–9905.
8. Nath, M.; Rao, C. N. R. New Metal Disulfide Nanotubes. *J. Am. Chem. Soc.* **2001,** *123*, 4841–4842.
9. Chen, J.; Li, S. L.; Xu, Q.; Tanaka, K. Synthesis of Open-Ended MoS_2 Nanotubes and the Application as the Catalyst of Methanation. *Chem. Commun.* **2002,** *16*, 1722–1723.
10. Chen, J.; Kuriyama, N.; Yuan, H. T.; Takeshita, H. T.; Sakai, T. Electrochemical Hydrogen Storage in MoS_2 Nanotubes. *J. Am. Chem. Soc.* **2001,** *123*, 11813–11814.
11. Nath, M.; Rao, C. N. R. Nanotubes of Group 4 Metal Disulfides. *Angew. Chem.* **2002,** *114*, 3601–3604.
12. Katz, A.; Redlich, M.; Rapoport, L.; Wagner, H. D.; Tenne, R. Self-lubricating Coatings Containing Fullerene-like WS_2 Nanoparticles for Orthodontic Wires and Other Possible Medical Applications. *Tribol. Lett.* **2006,** *21*, 135–139.
13. Redlich, M.; Katz, A.; Rapoport, L.; Wagner, H. D.; Feldman, Y.; Tenne, R. Improved Orthodontic Stainless Steel Wires Coated with Inorganic Fullerene-like Nanoparticles of WS_2 Impregnated in Electroless Nickel−phosphorous Film. *Dent. Mater.* **2008,** *24*, 1640–1646.
14. Samorodnitzky-Naveh, G. R.; Redlich, M.; Rapoport, L.; Fedman, Y.; Tenne, R. Inorganic Fullerene-like Tungsten Disulfide Nanocoating for Friction Reduction of Nickel-titanium Alloys. *Nanomedicine (London, U. K.)* **2009,** *4*, 943–950.
15. Tahir, M. N.; Yella, A.; Sahoo, J. K.; Annal-Therese, H.; Zink, N.; Tremel, W. Synthesis and Functionalization of Chalcogenide Nanotubes. *Phys. Status Solidi B* **2010,** *247*, 2338–2363.
16. Tsabari, H. *Final report*, Batch no. HP6, Harlan Biotech: Rehovot, Israel, 2005.
17. Haist, I. Test for Sensitization (Local Lymph Node Assay - LLNA) with Inorganic Fullerene-like WS2 Nanospheres. *Project No. 052052*, BSL Disservice, Germany, 2005.
18. Moore, G. E. Acute Inhalation Toxicity Study in Rats-Limit Test. *Study No. 18503*, Product Safety Laboratories: Dayton, NJ, USA, 2006.
19. Tenne, R.; Homyonfer, M.; Feldman, Y. Nanoparticles of Layered Compounds with Hollow Cage Structures (Inorganic Fullerene-Like Structures). *Chem. Mater.* **1998,** *10*, 3225–3238.
20. Tenne, R. Inorganic Nanotubes and Fullerene-Like Materials. *Chem.—Eur. J.* **2002,** *8*, 5296–5304.
21. Zak, A.; Feldman, Y.; Alperovich, V.; Rosentsveig, R.; Tenne, R. Growth Mechanism of MoS_2 Fullerene-like Nanoparticles by the Gas Phase Synthesis. *J. Am. Chem. Soc.* **2000,** *122*, 11108–11116.
22. Zelenski, C. M.; Dorhout, P. K. Template Synthesis of Near-Monodisperse Microscale Nanofibers and Nanotubules of MoS_2. *J. Am. Chem. Soc.* **1998,** *120*, 734–742.
23. Nath, M.; Govindaraj, A.; Rao, C. N. R. Simple Synthesis of MoS_2 and WS_2 Nanotubes. *Adv. Mater.* **2001,** *13*, 283–286.
24. Hsu, W. K.; Chang, B. H.; Zhu, Y. Q.; Han, W. Q.; Terrones, H.; Terrones, M.; Grobert, N.; Cheetham, A. K.; Kroto, H. W.; Walton, D. R. M. An Alternative Route to Molybdenum Disulfide Nanotubes. *J. Am. Chem. Soc.* **2000,** *122*, 10155–10158.
25. Remskar, M.; Mrzel, A.; Skraba, Z.; Jesih, A.; Ceh, M.; Demsar, J.; Stadelmann, P.; Levy, F.; Mihailovic, D. Self-Assembly of Subnanometer-Diameter Single-Wall MoS_2 Nanotubes. *Science* **2001,** *292*, 479–481.
26. Li, Q.; Newberg, J. T.; Walter, E. C.; Hemminger, J. C.; Penner, R. M. Polycrystalline Molybdenum Disulfide (2H-MoS_2) Nano- and Microribbons by Electrochemical/Chemical Synthesis. *Nano Lett.* **2004,** *4*, 277–281.
27. Morandi, V.; Marabelli, F.; Amendola, V.; Meneghetti, M.; Comoretto, D. Light Localization Effect on the Optical Properties of Opals Doped with Gold Nanoparticles. *J. Phys. Chem. C* **2008,** *112*, 6293.
28. Nath, M.; Rao, C. N. R.; Popovitz-Biro, R.; Albu-Yaron, A; Tenne, R. Nanoparticles Produced by Laser Ablation of HfS_3 in Liquid Medium: Inorganic Fullerene-Like Structures of Hf_2S. *Chem. Mater.* **2004,** *16*, 2238–2243.
29. Rapoport, L.; Fleischer, N.; Tenne, R. Applications of WS_2 (MoS_2) Inorganic Nanotubes and Fullerene-like Nanoparticles for Solid Lubrication and for Structural Nanocomposites. *J. Mater. Chem.* **2005,** *15*, 1782–1788.
30. Feldman, Y.; Wasserman, E.; Srolovitz, D. J.; Tenne, R. High-Rate, Gas-Phase Growth of MoS_2 Nested Inorganic Fullerenes and Nanotubes. *Science* **1995,** *267*, 222–225.

31. Stacy, A. M.; Hodul, D. T. Raman spectra of IVB and VIB Transition Metal Disulfides Using Laser Energies Near the Absorption Edges. *J. Phys. Chem. Solids.* **1985,** *46*, 405–409.
32. Frey, G. L.; Tenne, R.; Matthews, M. J.; Dresselhaus, M. S.; Dresselhaus, G. Raman and Resonance Raman Investigation of MoS_2 Nanoparticles. *Phys. Rev. B: Condens. Matter Mater. Phys.* **1999,** *60*, 2883–2892.
33. Li, X.; Ge, J.; Li, Y. Atmospheric Pressure Chemical Vapor Deposition: An Alternative Route to Large-Scale MoS_2 and WS_2 Inorganic Fullerene-like Nanostructures and Nanoflowers. *Chem.—Eur. J.* **2004,** *10*, 6163–6171.
34. Virsek, M.; Jesih, A.; Milosevic, I.; Damnjanovic, M.; Remskar, M. Raman scattering of the MoS_2 and WS_2 Single Nanotubes. *Surf. Sci.* **2007,** *601*, 2868–2872.
35. Kelly, R.; Cuomo, J. J.; Leary, P. A.; Rothenberg, J. E.; Braren, B. E.; Aliotta, C. F. Laser sputtering: Part I. On the Existence of Rapid Laser Sputtering at 193 nm. *Nucl. Instrum. Methods Phys. Res., Sect. B* **1985,** *9*, 329.
36. Manna, S. K.; Sarkar, S.; Barr, J.; Wise, K.; Barrera, E. V.; Jejelowo, O.; Rice-Ficht, A. C.; Ramesh, G. T. Single-walled Carbon Nanotube Induces Oxidative Stress and Activates Nuclear Transcription Factor-rB in Human Keratinocytes. *Nano Lett.* **2005,** *5*, 1676–1684.